

# Parametric resonance in quantum field theory

Jürgen Berges and Julien Serreau

*Institut für Theoretische Physik, Philosophenweg 16, 69120 Heidelberg, Germany*

We present the first study of parametric resonance in quantum field theory from a complete next-to-leading order calculation in a systematic  $1/N$  expansion, which includes scattering and memory effects. The far-from-equilibrium dynamics is solved numerically for an  $O(N)$ -symmetric scalar theory in  $3+1$  dimensions. We find that the classical resonant amplification at early times is followed by a collective amplification regime with explosive particle production in a broad momentum range, which is not accessible in a leading-order calculation. As a consequence, one observes rapid prethermalization with a particle number distribution monotonous in momentum.

In classical mechanics parametric resonance is the phenomenon of resonant amplification of the amplitude of an oscillator having a time-dependant periodic frequency. In the context of quantum field theory a similar phenomenon describes the amplification of quantum fluctuations, which can be interpreted as particle production. It provides an important building block for our understanding of the (pre)heating of the early universe after a period of inflation [1]. It may also be operative in the context of relativistic heavy-ion collisions in the formation of disoriented chiral condensates [2], or the decay of Polyakov loop condensates [3], or parity-odd bubbles [4].

Parametric resonance is a far-from-equilibrium phenomenon involving the production of particles with densities inversely proportional to the coupling. The non-perturbatively large occupation numbers cannot be described by standard kinetic approaches, employing resummed (two-particle irreducible) loop expansions. So far, classical field theory studies on the lattice have been the only quantitative approach available [5]. These are expected to be valid for not too late times, before the approach to quantum thermal equilibrium sets in. Up to now, studies in quantum field theory have been limited to mean-field type approximations (leading-order in large- $N$ , or Hartree) which neglect scatterings [6]. These approximations are known to fail to describe late-time thermalization and, even at early times, may not give a valid description of the entire amplification regime [7].

In this work, we study parametric resonance in quantum field theory at next-to-leading order (NLO) in a systematic two-particle irreducible ( $2PI$ )  $1/N$  expansion [8,9]. The nonperturbative expansion in the number of field components  $N$  can provide a small parameter even for extreme nonequilibrium situations. The  $2PI$ - $1/N$  expansion at NLO has been successfully employed previously for the description of far-from-equilibrium dynamics and thermalization in  $1+1$  dimensional quantum field theories [8]. The present calculations provide for the first time results in  $3+1$  dimensions, relevant for realistic particle physics applications.

We consider a real scalar  $N$ -component quantum field  $\varphi_a$  ( $a = 1, \dots, N$ ) with  $\lambda/(4!N) (\varphi_a \varphi_a)^2$  interaction, where summation over repeated indices is implied. All correlation functions of the quantum theory can be ob-

tained from the  $2PI$  generating functional for Green's functions  $\Gamma[\phi, G]$ , parametrized by the field expectation value  $\phi_a(x) = \langle \varphi_a(x) \rangle$  and the connected propagator  $G_{ab}(x, y) = \langle \varphi_a(x) \varphi_b(y) \rangle - \phi_a(x) \phi_b(y)$  [10]:

$$\Gamma[\phi, G] = S[\phi] + \frac{i}{2} \text{Tr} \ln G^{-1} + \frac{i}{2} \text{Tr} G_0^{-1}(\phi) G + \Gamma_2[\phi, G].$$

Here  $iG_{0,ab}^{-1}(x, y; \phi) \equiv \delta^2 S[\phi] / \delta \phi_a(x) \delta \phi_b(y)$ , where  $S$  is the classical action with  $S_0 = -\int_x \phi_a(\square_x + m^2) \phi_a / 2$  as the free part. We use the notation  $\int_x \equiv \int_{\mathcal{C}} dx^0 \int d\mathbf{x}$  with  $\mathcal{C}$  denoting a closed time path along the real axis. At NLO in the  $2PI$ - $1/N$  expansion one finds [9,8]

$$\Gamma_2[\phi, G] = \frac{i}{2} \text{Tr}_{\mathcal{C}} \text{Ln}[\mathbf{B}(G)] + \frac{i\lambda}{6N} \int_{xy} \mathbf{I}(x, y; G) \phi_a(x) G_{ab}(x, y) \phi_b(y), \quad (1)$$

$$\mathbf{B}(x, y; G) = \delta_{\mathcal{C}}(x - y) + i \frac{\lambda}{6N} G_{ab}(x, y) G_{ab}(x, y), \quad (2)$$

$$\mathbf{I}(x, y; G) = \frac{\lambda}{6N} G_{ab}(x, y) G_{ab}(x, y) - i \frac{\lambda}{6N} \int_z \mathbf{I}(x, z; G) G_{ab}(z, y) G_{ab}(z, y). \quad (3)$$

The equations of motion for  $\phi_a$  and  $G_{ab}$  are given by [10]

$$\frac{\delta \Gamma[\phi, G]}{\delta \phi_a(x)} = 0 \quad , \quad \frac{\delta \Gamma[\phi, G]}{\delta G_{ab}(x, y)} = 0. \quad (4)$$

The resulting evolution equations have been derived in detail in [9,8]. (More precisely, we employ the equations displayed in Eqs. (5.1) and (B.6) - (B.14) of [9].) We solve them numerically on a lattice along the lines of [8], and all expressions below are understood to be regularized by the lattice. Typical volumes  $(N_s a_s)^3$  of  $N_s = 36-48$  with  $a_s = 0.4-0.3$  lead to results insensitive to finite-size and cutoff effects. Displayed numerical results are for  $N = 4$ .

*Initial conditions.* We consider an initial system in a pure quantum state. We employ spatially homogeneous fields  $\phi_a(t) = \sigma(t) M_0 \sqrt{6N/\lambda} \delta_{a1}$ , where  $M_0$  sets our unit of mass defined below, with  $\sigma(0) = \sigma_0$  and  $\partial_t \sigma(t)|_{t=0} = 0$ . The initial propagator is taken to be diagonal with  $G_{ab} = \text{diag}\{G_{\parallel}, G_{\perp}, \dots, G_{\perp}\}$ . Fourier transformed with

respect to the spatial coordinates one has to specify the longitudinal and transverse modes  $G_{\parallel,\perp}(t, t'; \mathbf{p})$  and their first time derivatives at  $t = t' = 0$ . To separate the real and imaginary part we write  $G_{\parallel}(t, t'; \mathbf{p}) = F_{\parallel}(t, t'; \mathbf{p}) - \frac{i}{2} \rho_{\parallel}(t, t'; \mathbf{p}) \text{sign}_c(t - t')$  and equivalently for  $G_{\perp}$  [8]. The time-antisymmetric real function  $\rho_{\parallel,\perp}$  denotes the spectral function proportional to the commutator of two fields, and  $F_{\parallel,\perp}$  is the real symmetric propagator. Initially,  $F_{\parallel}(0, 0; \mathbf{p}) = 1/2\omega_{\parallel}(\mathbf{p})$ ,  $\partial_t F_{\parallel}(t, 0; \mathbf{p})|_{t=0} = 0$  and  $\partial_t \partial_{t'} F_{\parallel}(t, t'; \mathbf{p})|_{t=t'=0} = \omega_{\parallel}(\mathbf{p})/2$ ; equivalently for  $F_{\perp}$ . The initial frequencies are  $\omega_{\parallel}(\mathbf{p}) = [\mathbf{p}^2 + M_0^2(1 + 3\sigma_0^2)]^{1/2}$ ,  $\omega_{\perp}(\mathbf{p}) = [\mathbf{p}^2 + M_0^2(1 + \Delta_0 + \sigma_0^2)]^{1/2}$  with  $M_0^2 \equiv M^2(0)$  and  $\Delta_0 = \lambda[T_{\perp}(0) - T_{\parallel}(0)]/3N$ , where we define

$$M^2(t) = m^2 + \frac{\lambda}{6N} [3T_{\parallel}(t) + (N-1)T_{\perp}(t)], \quad (5)$$

$$T_{\parallel,\perp}(t) = \int \frac{d\mathbf{p}}{(2\pi)^3} F_{\parallel,\perp}(t, t; \mathbf{p}). \quad (6)$$

The initial conditions for the spectral functions are fixed by the equal-time commutation relations:  $\rho_{\parallel,\perp}(t, t'; \mathbf{p})|_{t=t'} = 0$  and  $\partial_t \rho_{\parallel,\perp}(t, t'; \mathbf{p})|_{t=t'} = 1$ . We define the effective particle numbers

$$n_{\parallel,\perp}(\mathbf{p}) + \frac{1}{2} = [F_{\parallel,\perp}(t, t'; \mathbf{p}) \partial_t \partial_{t'} F_{\parallel,\perp}(t, t'; \mathbf{p})]_{t=t'}^{1/2} \quad (7)$$

and associated mode energies as in [8,11]. For  $\phi = 0$  these definitions have been shown to yield an efficient quasiparticle interpretation for the  $O(N)$ -model and to approach a Bose-Einstein distributed particle number at sufficiently late times [8,11]. In the following, all quantities are rescaled with appropriate powers of  $M_0$  to become dimensionless.

*Transition between classical field and fluctuation dominated regime.* The above initial conditions are characterized by zero particle number densities and large field amplitudes for small coupling  $\lambda$ . In this case the dominant contributions to  $\Gamma$  at early times come from the classical action  $S \sim \lambda^{-1}$ . Correspondingly, the (conserved) total energy is well approximated by the classical field contribution, i.e.  $E_{\text{tot}} \simeq E_{\text{cl}}$ , as shown in Fig. 1. When the system evolves in time, more and more energy is converted into fluctuations. In the following we describe the corresponding characteristic regimes.

*(I) Early-time (Lamé) regime: classical parametric resonance.* At early times the  $\sigma$ -field evolution equation receives the dominant ( $\mathcal{O}(\lambda^0)$ ) contributions from the classical action  $S$ . As a consequence, the field dynamics can be described by the classical equation of motion. The evolution equations for the two-point functions at  $\mathcal{O}(\lambda^0)$  correspond to free-field equations with the addition of a time dependent mass term  $\sim 3\sigma^2(t)$  for the longitudinal and  $\sim \sigma^2(t)$  for the transverse modes.

The dynamics in this approximation has been extensively studied in the literature and is known to be described by the solution of the Lamé equation [1,6]. Parametric resonance leads to an exponential growth of two-point correlation functions. As described in detail in [6],

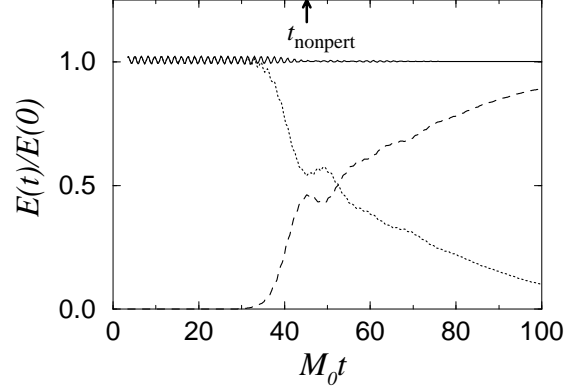


FIG. 1. Total energy (solid line) and classical field energy (dotted line) as a function of time for  $\lambda = 10^{-6}$ . The dashed line represents the fluctuation part, showing a transition between a classical field and a fluctuation dominated regime.

resonant amplification occurs for the *transverse* modes in the momentum range  $0 \leq \mathbf{p}^2 \leq \sigma_0^2/2$ , and the maximally amplified mode is  $p = p_0 \simeq \sigma_0/2(1 - \delta)$ . Here the small positive number  $\delta \leq e^{-\pi}$  [6], and for the initial value  $\sigma_0 = 2$  employed here one has  $\delta \simeq 3.2 \times 10^{-2}$ . There is a clear separation of scales between the maximum amplification rate,  $\gamma_0 \simeq 4\delta\sqrt{1 + \sigma_0^2}(1 - 4\delta)$ , and the characteristic oscillation frequency of the modes,  $\omega_0 \simeq \sqrt{1 + \sigma_0^2}(1 - 4\delta)$ . For use below, the second derivative of the amplification rate with respect to momentum at  $p = p_0$  is  $\gamma_0'' \simeq -32\delta\sqrt{1 + \sigma_0^2}(1 - 6\delta)$ . Averaging over the short time scale  $\sim \omega_0^{-1}$  one finds for  $t, t' \gg \gamma_0^{-1}$ :

$$F_{\perp}(t, t'; \mathbf{p}_0) \sim e^{\gamma_0(t+t')}. \quad (8)$$

For the *longitudinal* modes one observes a much smaller growth in a narrow momentum range centered around  $p \sim 3p_0$ . In this regime, the analytic results agree precisely with the NLO numerical results. Figs. 2 and 3 show the transverse and longitudinal particle numbers, averaged over the rapid oscillation time scale.

*(II) Source-induced amplification regime ( $t \simeq t_{\text{source}}$ ): strongly enhanced particle production for longitudinal modes.* Because of the exponential growth of the transverse fluctuations for  $\gamma_0 t \gg 1$ , the  $\mathcal{O}(\lambda^0)$  approximation breaks down at some time  $t_{\text{source}}$ , which will be shown to happen when  $F_{\perp}(t, t'; \mathbf{p}_0) \simeq \mathcal{O}(N^0 \lambda^{-1/2})$ : At  $\mathcal{O}(\lambda)$  the evolution equation (4) for  $F_{\parallel}$  can be approximated by

$$\begin{aligned} & \left( \partial_t^2 + \mathbf{p}^2 + M^2(t) + 3\sigma^2(t) \right) F_{\parallel}(t, t'; \mathbf{p}) \simeq \\ & \frac{2\lambda(N-1)}{3N} \sigma(t) \left\{ \int_0^t dt'' \sigma(t'') \Pi_{\perp}^{\rho}(t, t''; \mathbf{p}) F_{\parallel}(t'', t'; \mathbf{p}) \right. \\ & \left. - \frac{1}{2} \int_0^{t'} dt'' \sigma(t'') \Pi_{\perp}^F(t, t''; \mathbf{p}) \rho_{\parallel}(t'', t'; \mathbf{p}) \right\}, \quad (9) \end{aligned}$$

$\Pi_{\perp}^A(t, t''; \mathbf{p}) = \int d\mathbf{q}/(2\pi)^3 F_{\perp}(t, t''; \mathbf{p} - \mathbf{q}) A_{\perp}(t, t''; \mathbf{q})$ , with  $A \equiv F, \rho$ . Here we have used the fact that the  $\Pi$ -self-energies are dominated by the transverse fluctuations and, similarly, we note that  $T_{\perp} \gg T_{\parallel}$  in the mass

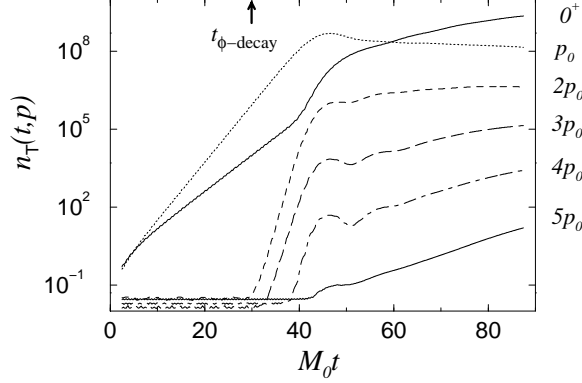


FIG. 2. Effective particle number density for the transverse modes as a function of time for various momenta  $0 \leq p \leq 5p_0$  and  $\lambda = 10^{-6}$ . At times  $t \lesssim t_{\text{nonpert}}$  there is exponential amplification with rate  $\sim 2\gamma_0$  for  $p \simeq p_0$ . An enhanced rate  $\sim 6\gamma_0$  sets in for  $t \gtrsim t_{\phi\text{-decay}}$  affecting a broad momentum range.

term (5). In addition, we used that  $F_{\perp}^2(t, t''; \mathbf{p}_0) \gg \rho_{\perp}^2(t, t''; \mathbf{p}_0)/4$  for  $t'' \simeq t$ . We stress that the latter inequality represents a sufficient condition for the suppression of quantum fluctuations in this regime [8]. Its validity can be seen from the early-time behavior (8) and the corresponding one of  $\rho_{\perp}(t, t''; \mathbf{p}_0) \sim e^{\gamma_0(t-t'')}$  for  $t'' \lesssim t$ .

*Memory expansion:* Because of the exponential growth, the dominant contributions to the memory integrals in (9) come from latest times  $t'' \simeq t, t'$ . Exploiting the clear separation of scales  $\omega_0^{-1} \ll \gamma_0^{-1}$ , we note that due to the periodic behavior of the rapidly oscillating part of the unequal-time two-point functions, an approximate description needs only integration over one period of oscillation  $\sim 2\pi/\omega_0$ . From the explicit early-time behavior for the dominant modes [6], one finds that it is sufficient to evaluate the memory integrals over a fourth of a period:  $t - \pi/2\omega_0 \lesssim t'' \leq t$ . Indeed, we have verified numerically to high accuracy that, in this regime, one can replace  $\int_0^t dt'' \rightarrow \int_{t-c/\omega_0}^t dt''$  with constant  $c \sim 1$ . Using this effective locality one may expand the integrands around the upper bounds  $t$  and  $t'$ . With  $\rho_{\parallel, \perp}(t, t''; \mathbf{p}) \simeq \partial_{t''} \rho_{\parallel, \perp}(t, t''; \mathbf{p})|_{t=t''} (t'' - t) \equiv (t - t'')$ , we obtain for the first term on the RHS of (9):

$$\begin{aligned} & \lambda \sigma(t) \frac{2(N-1)}{3N} \int_{t-c/\omega_0}^t dt'' \sigma(t'') \Pi_{\perp}^{\rho}(t, t''; \mathbf{p}) F_{\parallel}(t'', t'; \mathbf{p}) \\ & \simeq \lambda \sigma^2(t) F_{\parallel}(t, t'; \mathbf{p}) \frac{c^2}{\omega_0^2} \frac{(N-1)}{3N} T_{\perp}(t). \end{aligned} \quad (10)$$

Similarly, the second term on the RHS yields

$$\begin{aligned} & -\lambda \sigma(t) \frac{(N-1)}{3N} \int_{t'-c/\omega_0}^{t'} dt'' \sigma(t'') \Pi_{\perp}^F(t, t''; \mathbf{p}) \rho_{\parallel}(t'', t'; \mathbf{p}) \\ & \simeq \lambda \sigma(t) \sigma(t') \frac{c^2}{\omega_0^2} \frac{(N-1)}{6N} \Pi_{\perp}^F(t, t'; \mathbf{p}). \end{aligned} \quad (11)$$

Here (10) reduces the mass term in the evolution equation for  $F_{\parallel}$ , whereas (11) represents a source term. Estimating  $T_{\perp}$  and  $\Pi_{\perp}^F$  in the above  $\mathcal{O}(\lambda)$ -equations, we can use

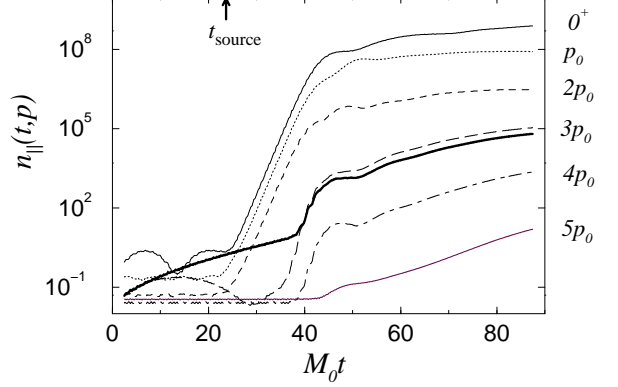


FIG. 3. Same as in Fig. 2, but for the longitudinal modes. The thick line shows the particle number for a mode in the parametric resonance band, and the long-dashed line for a similar one outside the band. At  $t \simeq t_{\text{source}}$  enhanced particle production with rate  $\sim 4\gamma_0$  sets in around  $0 \lesssim p \lesssim 2p_0$ .

the results from the Lamé regime. The momentum integrals are dominated by  $p \simeq p_0$  and can be evaluated for  $t \simeq t' \gg \gamma_0^{-1}$  using a saddle point approximation with  $F_{\perp}(t, t', \mathbf{p}) \simeq F_{\perp}(t, t', \mathbf{p}_0) \exp[-|\gamma_0''|(t+t')(p-p_0)^2/2]$ :

$$T_{\perp}(t) \simeq \frac{p_0^2 F_{\perp}(t, t; \mathbf{p}_0)}{4(\pi^3 |\gamma_0''| t)^{1/2}}, \quad (12)$$

$$\Pi_{\perp}^F(t, t'; 0) \simeq \frac{p_0^2 F_{\perp}^2(t, t'; \mathbf{p}_0)}{4(\pi^3 |\gamma_0''| (t+t'))^{1/2}}, \quad (13)$$

where we focus for the source term on its maximum at  $\mathbf{p} = 0$ . Averaging over the short time scale  $\sim \omega_0^{-1}$ , one has  $\sigma^2 \sim \sigma_0^2/2$  and  $F_{\parallel}(t, t; 0) \sim 1/\sqrt{1+3\sigma_0^2}$  as well as (8). An important characteristic time is reached when the LO large- $N$  corrections to the mass term in (5), and the NLO ones (10), become comparable to the classical mass term. For this to happen,  $T_{\perp} \simeq \mathcal{O}(\lambda^{-1})$  and with (8) the corresponding time is parametrically given by  $t_{\text{nonpert}} \simeq (\ln \lambda^{-1})/(2\gamma_0)$ . A detailed description at LO can be found in [6]. Note that here the LO and NLO contributions to the mass term are of the same order but with opposite sign. We point out that by comparing with the LHS of (9) one finds the source term (11) for the longitudinal modes to become important at the *earlier* time

$$t_{\text{source}} \simeq t_{\text{nonpert}}/2, \quad (14)$$

which agrees with the results in Fig. 5. For  $t \gtrsim t_{\text{source}}$  the Lamé description for the longitudinal modes is no longer valid and from (9), (11) one finds the strong amplification  $F_{\parallel}(t, t'; 0) \sim \exp[2\gamma_0(t+t')]$ , in accordance with Fig. 3.

(III) *Collective amplification regime* ( $t \simeq t_{\phi\text{-decay}}$ ): *exponential decrease of the classical field energy and explosive particle production in a broad momentum range.* A similar analysis than the one above can be made for the transverse fluctuations. Beyond the  $\mathcal{O}(\lambda^0)$  (Lamé) description, the evolution equation (4) for  $F_{\perp}$  receives contributions from the feed-back of the longitudinal modes at  $\mathcal{O}(\lambda)$  as well as from the amplified transverse mode

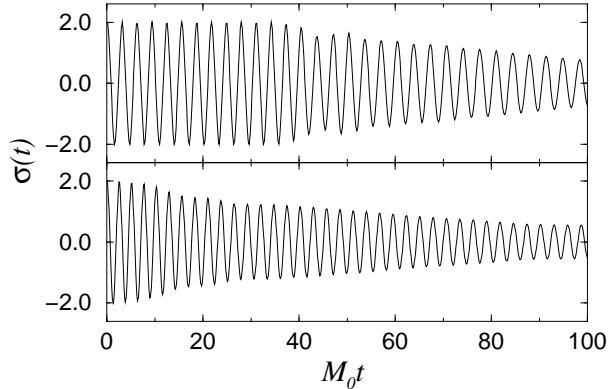


FIG. 4. The rescaled field  $\sigma$  as a function of time for  $\lambda = 10^{-6}$  (up) and  $\lambda = 10$  (below). For  $0 \leq t \lesssim t_{\phi\text{-decay}}(\lambda)$  the amplitude remains almost constant.

at  $\mathcal{O}(\lambda^2)$ . Both terms are (schematically) of the form  $\sim \lambda^2 F_{\perp}^3/N$ , which leads to the characteristic time

$$t_{\phi\text{-decay}} \simeq 2 t_{\text{nonpert}}/3 + (\ln N)/(6\gamma_0) \quad (15)$$

at which  $F_{\perp}(t, t'; \mathbf{p}_0) \simeq \mathcal{O}(N^{1/3} \lambda^{-2/3})$ . Correspondingly, for  $t_{\phi\text{-decay}} \lesssim t \lesssim t_{\text{nonpert}}$  there is a large particle production rate  $\sim 6\gamma_0$  for a wide range of momenta, in agreement with the full NLO results in Fig. 2. In this time range the longitudinal modes exhibit an enhanced amplification as well, shown in Fig. 3. The abundant particle production is accompanied by an exponential decrease of the classical field energy. Fig. 1 exhibits a very rapid transition to a stage with  $E_{cl} \simeq E_{\text{tot}}/2$  at  $t \simeq t_{\text{nonpert}}$ . We emphasize that the collective amplification regime is absent in the LO large- $N$  approximation. Consequently, the latter can only be valid until  $t_{\text{nonpert}}$  if  $t_{\phi\text{-decay}} \geq t_{\text{nonpert}}$ . Using (15) this translates into a lower parametrical bound for  $N$  below which LO breaks down:  $N \gtrsim \lambda^{-1}$ .

(IV) *Nonperturbative regime* ( $t \simeq t_{\text{nonpert}}$ ): *prethermalization*. As described above, at  $t \simeq t_{\text{nonpert}}$  one finds  $F_{\perp}(t, t'; \mathbf{p}_0) \simeq \mathcal{O}(N^0 \lambda^{-1})$ . As a consequence, there are leading contributions to the dynamics coming from all loop orders (cf. (1)–(3)). To describe this regime and the late-time behavior it is crucial to employ a nonperturbative approximation as provided by the  $1/N$  expansion at NLO [8,9]. In particular, the evolution equations are no longer “local” in the sense described under (II). In this regime we also observe small dependencies on the employed lattice spacings. In contrast, for  $t \lesssim t_{\text{nonpert}}$  the dynamics is dominated by modes much below the momentum cutoff and therefore insensitive to cutoff effects.

The fluctuation dominated regime is characterized by strong nonlinearities. For instance, from Fig. 1 one infers for  $t \simeq t_{\text{nonpert}}$  that the classical field decay “overshoots” and is temporarily reversed by feed-back from the modes. The short enhancement of the field can be directly seen in Fig. 4, and  $n_{\perp, \parallel}$  exhibits a corresponding reverse behavior in Figs. 2 and 3. Subsequent oscillations in the envelope of  $\sigma(t)$  become smaller with time, and from Figs. 4 and 1 one observes a slow decay of the field and  $E_{cl}$ .

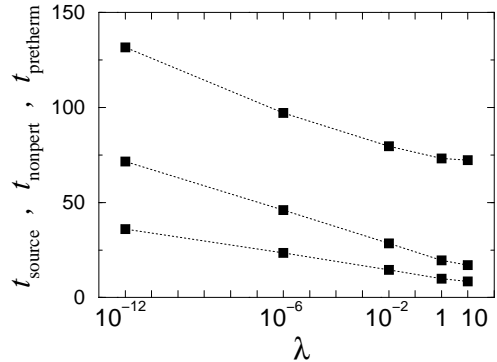


FIG. 5. The times  $t_{\text{source}}$ ,  $t_{\text{nonpert}}$  and  $t_{\text{pretherm}}$  as a function of  $\lambda$ . We find a rapid prethermalization with a monotonous ordering of modes at  $t \simeq t_{\text{pretherm}}$ .

Though the thermalization time is larger than  $t_{\text{nonpert}}$ , as can also be seen from the mismatch of  $n_{\perp}$  and  $n_{\parallel}$  in Figs. 2 and 3 at that time, we find a comparably rapid prethermalization to a monotonously decreasing particle number distribution as a function of momentum. After the time  $t_{\text{pretherm}}$ , shown in Fig. 5 as a function of  $\lambda$ , the *relative* ordering of the mode numbers  $n_{\perp, \parallel}(\mathbf{p})$  does not change. In the spirit of Refs. [2,12], for practical purposes many aspects at  $t_{\text{pretherm}}$  do not differ much from the late-time thermal regime. This will be discussed in a separate publication [13].

We thank R. Baier, C. Wetterich and T. Prokopec for fruitful discussions. Numerical computations were done on the PC cluster HELICS of the Interdisciplinary Center for Scientific Computing (IWR), Heidelberg University.

- 
- [1] J.H. Traschen and R.H. Brandenberger, Phys. Rev. D **42**, 2491 (1990); L. Kofman, A.D. Linde and A.A. Starobinsky, Phys. Rev. Lett. **73**, 3195 (1994).
  - [2] S. Mrowczynski, B. Müller, Phys. Lett. B **363**, 1 (1995).
  - [3] A. Dumitru and R. D. Pisarski, Phys. Lett. B **504**, 282 (2001).
  - [4] D. Ahrensmeier, R. Baier and M. Dirks, Phys. Lett. B **484**, 58 (2000).
  - [5] S.Yu. Khlebnikov and I.I. Tkachev, Phys. Rev. Lett. **77**, 219 (1996); T. Prokopec and T.G. Roos, Phys. Rev. D **55**, 3768 (1997).
  - [6] D. Boyanovsky, H.J. de Vega, R. Holman and J.F.J. Salgado, Phys. Rev. D **54**, 7570 (1996).
  - [7] L. Kofman, A.D. Linde and A.A. Starobinsky, Phys. Rev. D **56**, 3258 (1997).
  - [8] J. Berges, Nucl. Phys. **A699**, 847 (2002); G. Aarts and J. Berges, Phys. Rev. Lett. **88**, 041603 (2002).
  - [9] G. Aarts, D. Ahrensmeier, R. Baier, J. Berges and J. Serreau, to appear in Phys. Rev. D (hep-ph/0201308).
  - [10] J. M. Cornwall, R. Jackiw and E. Tomboulis, Phys. Rev. D **10**, 2428 (1974).
  - [11] J. Berges and J. Cox, Phys. Lett. B **517**, 369 (2001); G. Aarts and J. Berges, Phys. Rev. D **64**, 105010 (2001).
  - [12] G.F. Bonini and C. Wetterich, Phys. Rev. D **60**, 105026 (1999).
  - [13] J. Berges, J. Serreau and C. Wetterich, in preparation.